



Binding mechanism of strontium to biopolymer hydrogel composite materials

Stella Foster¹ · Nitya Ramanan² · Bruce Hanson¹ · Bhoopesh Mishra³

Received: 20 July 2022 / Accepted: 4 October 2022 / Published online: 9 November 2022
© The Author(s) 2022

Abstract

Strontium-90 is a radionuclide of concern that is mobile in soil and groundwater and is a threat to life. Activated hydrogel biopolymer composites were fabricated for strontium remediation from groundwater. Batch uptake demonstrated a maximal strontium uptake capacity of 109 mg g⁻¹, much higher than unactivated hydrogel controls. Activation also more than doubled the decontamination factor at environmentally relevant concentrations. EXAFS was used to investigate the binding mechanism, revealing inner sphere complexation of strontium for the first time. Biopolymer composites synthesized for these studies are sustainable and cheap remediation materials that exhibit good strontium uptake and inner sphere binding.

Keywords Inner sphere complexation · Strontium EXAFS · Biopolymer · Biochar · Alginate · Radionuclide remediation

Introduction

Radio strontium is a challenging radionuclide to remediate and continues to pose challenges at a number of waste processing sites and sites of accidental release. As a major fission product it is present in large quantities in the form of Sr-89 and Sr-90 in the event of accidental release to the environment. For example, after the Chernobyl incident an estimated 10 PBq is thought to have been released [1] while following a tank leak in 2011 at the Fukushima Daiichi site, an estimated 45 TBq 90Sr [2, 3] released to a drainage ditch. It can also be detected in soils at > 50% of the United States Department of Energy sites and some of these sites exceed safe 90Sr concentrations in groundwater by as much as five orders of magnitude [4]. Typical groundwater strontium concentrations can vary considerably [5]. Strontium's electronic similarity with bio-essential calcium means that it is taken up readily by organisms where it accumulates in bones. Of particular concern is strontium-90 with a half-life

of 28.8 years, decaying via an energetic beta-emission and causing cancer [1] and leukaemia [2]. Strontium is soluble and relatively mobile in aqueous environments and it generally retains its hydration shell at environmentally relevant pH, tending to form outer sphere complexes with a range of inorganic materials [3–5]. Outer sphere complexation is characterised by a binding mediated through the hydration shell, which is a weak and reversible interaction. This behaviour makes strontium particularly challenging to immobilise. Inner sphere complexation by contrast, is characterised by partial or total loss of the hydration shell and a direct complexation or binding between strontium and surface oxygen groups—a far stronger electrostatic interaction and highly desirable in a remediation material.

In addition to the challenges posed by strontium's chemistry, groundwater contains a complex mixture of organics, inorganics and microbiota [6–9], all of which can rapidly foul microporous adsorbents blocking their pore structure and reducing their efficacy at immobilisation of strontium, in seawater, acidic waters and groundwater [10, 11]. Biopolymers, derived via biosynthesis, contain extensive multi-scale porosity which is not subject to the same issues of leaching and fouling as some inorganic ion-exchange materials. They are economically sustainable, can be prepared rapidly and are a step closer to carbon neutral or even carbon negative materials.

Alginate derived from brown kelp is an anionic biopolymer with abundant carboxylate and hydroxyl functionality

✉ Stella Foster
pmsjf@leeds.ac.uk

¹ School of Process and Chemical Engineering, University of Leeds, 211 Clarendon Road, Leeds LS2 9JT, UK

² Diamond Light Source, Harwell Science and Innovation Campus, Didcot OX11 0DE, UK

³ Physics Department, Illinois Institute of Technology, 10 West 35th Street, Chicago, IL 60616, USA

well suited for cation complexation. It also has well characterised gelation properties [12], able to form monolithic hydrogels. Biochar is another such carbonaceous material derived from ligno-cellulosic residues, which is well suited to cation immobilisation due to extensive porosity and surface oxygen functionality. Biochar can be activated by chemical or physical agents to enhance both its porosity and surface functional chemistry useful for adsorptive processes, further increasing its contaminant uptake capacity. Due to their amorphous structure, elucidating the binding mechanism of strontium to biopolymers such as biochar is, however, challenging. Characterising the binding mechanism is crucial for proving that biopolymers are effective at immobilising strontium effectively. Extended X-ray Absorption fine Structure (EXAFS) is one such technique that has been employed to successfully elucidate the binding environment of a range of metals adsorbed to surfaces [13, 14]. While a number of EXAFS studies have examined strontium binding environment in a range of inorganic materials, very few studies show direct proof of inner sphere binding [15, 16], and we are unaware of any previous EXAFS study on biopolymer adsorbents examining the binding mechanism of strontium.

Experimental

Sample preparation

Oakwood chips ($d < 3$ mm) were rinsed in de-ionized water before being dried overnight at 90 °C. They were pyrolysed at 450 °C (ramp = 5 °C min⁻¹, dwell 1 h) before being ball milled and sieved to < 50 µm in diameter. Unactivated control biochar was labelled 'OK'.

Activation followed a previously described and optimized procedure [17] briefly, milled biochar was treated with 8 M HNO₃ solution at 80 °C for three hours, then filtered, washed and dried at 105 °C overnight. Activated biochar was labelled 'OK-A'.

Hydrogel alginate-biochar beads were fabricated using previously described procedure [18]. Briefly, sodium alginate was dissolved in 99 mL of ultrapure water before biochar was added in a 1:0.25 ratio and the mixture was stirred for a further 24 h at 25 °C. The biochar-alginate slurry was added dropwise to a slowly stirring solution of a 0.1 M calcium chloride solution (500 mL). The resulting Biochar-alginate hydrogel beads were left to equilibrate for overnight before being rinsed thoroughly with ultrapure water and freeze-dried for 24 h. Samples were labelled 'HG' for hydrogel from unactivated biochar and 'HG-A' for hydrogel with activated biochar.

Uptake experiments

0.2 g of adsorbent was precisely weighed into a sterile 50 mL centrifuge tube, before 2 mL of a 0.2 M MOPS (3-(N-morpholino)propanesulfonic acid) buffer was added and the system left to equilibrate for 12 h. Aliquots of a 1000 mg L⁻¹ Sr²⁺ stock solution (from SrCl₂·6H₂O) were added before each tube was made up to 25 mL using a 0.2 M MOPS buffer solution (pH 7). Initial concentrations were between 5 and 500 mg L⁻¹ Sr²⁺ in a 0.2 M MOPS buffered solution. Samples were shaken at 150 rpm (24 h) before being filtered through a 0.45 µm cellulose syringe filter. The remaining solution was acidified to 2% nitric acid and the remaining Sr²⁺ concentration measured via ICP-MS.

Equilibrium loading q_e was derived using Eq. 1, where C_i and C_e are solution initial and equilibrium concentration (mg L⁻¹), V is volume of solution (L) and m is mass of adsorbent (g).

$$q_e = \frac{(C_i - C_e)V}{m} \quad (1)$$

The non-linear versions of the Langmuir (Eq. 2) and Freundlich (Eq. 3) isotherm models were employed and compared. The Langmuir equation takes the form:

$$q_e = \frac{q_m K_L C_e}{1 + K_L C_e} \quad (2)$$

where q_e and q_m describe the adsorption capacity at equilibrium and adsorption capacity respectively (mg g⁻¹), K_L is the Langmuir constant and C_e the equilibrium solution concentration (mg L⁻¹) [19]. The Freundlich equation describes heterogeneous sites of differing affinity:

$$q_e = k_F C_e^{1/n} \quad (3)$$

where k_F is the Freundlich constant and $1/n$ is the heterogeneity factor.

The decontamination factor, DF is derived by eqn the initial strontium concentration divided by the final strontium concentration.

$$DF = \frac{[Sr^{2+}]_i}{[Sr^{2+}]_f} \quad (4)$$

X-ray absorption spectroscopy

Strontium-loaded samples were retained from batch uptake experiments. Samples were rinsed in 15 mL UHQ on filter paper to remove any surface precipitated strontium. Samples were then dried overnight at 105 °C before being milled

and pressed into pellets using 20% cereox binder. EXAFS spectra were collected at B18, Diamond Light Source, UK. The strontium K-edge (16,105 eV) was measured at 77 K using a Si(111) monochromator. X-ray energy was calibrated using an yttrium foil. The Demeter package was used for data reduction & background removal before fitting of the Fourier transform. A shell-by-shell approach to fitting was undertaken in order to examine the degree of inner or outer sphere complexation [15]. Fitting of standards yielded an optimum value of S_0^2 to be 1.0 ± 0.03 .

Results and discussion

Strontium uptake

Results show that activation of oak wood biochar enhances strontium uptake capacity by around 100%. This is consistent with previous studies which show that activation enhances surface functional groups—particularly oxygen containing surface functional groups—that participate in cation complexation and immobilisation such as carboxylate and hydroxylate groups [20, 21]. For oxyphilic strontium, such functional groups play a crucial role in the uptake and complexation of contaminants. Encapsulation of unactivated biochar into hydrogel beads (HG) also enhanced uptake by around 50%. The alginate hydrogel provides additional binding sites for strontium thanks to its abundant carboxylate and hydroxyl functionality. It is the combination of activation and hydrogel encapsulation that produced the highest uptake overall (HG-A). Uptake was almost four times greater in the activated hydrogel over unactivated oak wood biochar control at an initial Sr^{2+} concentration of 500 mg L^{-1} . While biochar encapsulation in alginate hydrogel beads has previously been demonstrated to enhance strontium uptake [6], the addition of an activation step prior to hydrogel encapsulation, to our knowledge, has not yet been reported. Such a combination of activation and hydrogel formation appears to increase not only overall uptake capacity (Table 1) but also the binding affinity of binding sites, as evidenced by the increasing decontamination factor DF at contamination-relevant concentration levels (Table 2).

Table 1 shows isotherm modelling parameters for HG- and HG-A. The maximum uptake (Q_{MAX}) values are 108.5 mg g^{-1} for HG-A and 35.5 mg g^{-1} for HG. Uptake values for similar materials vary widely e.g. 120 mg g^{-1} for

Table 2 Decontamination factors (Eq. 4) for hydrogel composites and biochar control adsorbents at $[Sr^{2+}]_i = 5 \text{ mg L}^{-1}$

Sample	DF
HG-A	4.1 ± 0.005
HG	1.8 ± 0.074
OK-A	3.8 ± 0.008
OK	1.3 ± 0.006

a rice straw biochar [22], 12 mg g^{-1} for an activated sewage biochar [23] and 82 mg g^{-1} for a chitosan-alginate-yeast bead [29]. The adsorbents in this study are comparable with these values.

Figure 1 shows that none of the samples reach saturation Sr loading by the upper initial concentration of 500 mg L^{-1} , implying all have more unoccupied binding sites available.

Typically, data sets for isotherm modelling can reach as high as $10,000 \text{ mg L}^{-1}$ initial ion concentration in order to reach saturation binding. It should be noted that this dataset is not yet optimised for uptake capacity but rather was optimised in preparation for EXAFS binding mechanism studies and therefore the initial concentration range deliberately did not extend above 500 mg L^{-1} initial concentration. In real-world remediation scenarios, the concentration of radio strontium in groundwater is unlikely to reach beyond this level and the objective was to obtain EXAFS measurements that mimicked realistic potential contamination scenarios, while balancing the signal-to-noise of X-ray absorption transmission detectors. Further uptake studies are required which reach higher initial strontium concentration in order to obtain improved isotherm model fits. The source of the discontinuity of HG-A (Fig. 1) at around 50 mg L^{-1} initial Sr^{2+} concentration is not yet fully understood and is the subject of further investigation. Control experiments indicate no significant instrumental deviation, therefore likely explanations include a possible change in the binding mechanism at about 50 mg L^{-1} .

Extended X-ray absorption fine structure

Figure 2 shows the backscattering signals of samples HG-A, HG & OK-A as well as standard compounds of known crystallographic structure. Unactivated biochar (OK) was not analysed due to its poor uptake performance. As is typical of strontium K-edge EXAFS, the signal is dominated by a large and broad first peak, corresponding to the backscattering from first shell oxygen atoms surrounding strontium

Table 1 Isotherm modelling parameters for hydrogel and activated hydrogel composites

	Langmuir			Freundlich		
	Q_{MAX} (mg/g)	K (L/mg)	R^2	K_f (mg/g)	n	R^2
HG-A	108.5	0.003	0.9631	0.5553	0.8099	0.9915
HG	35.5	0.004	0.9914	0.6468	0.4897	0.9796

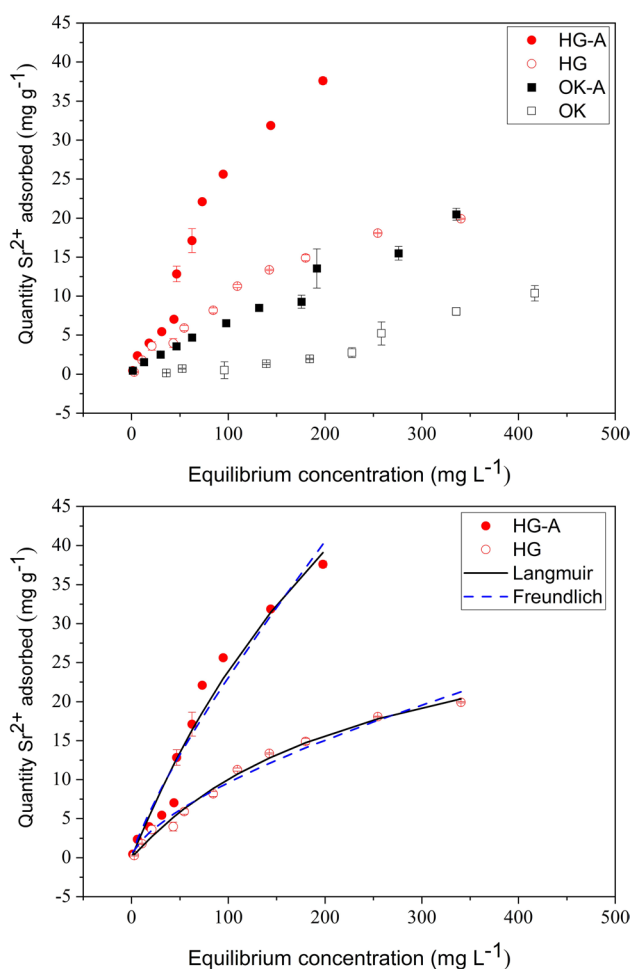


Fig. 1 Strontium batch uptake data (top) and isotherm modelling for hydrogel and activated hydrogel composites (bottom) buffered at pH7 for 24 h; 0.2 g adsorbent in 25 mL. Samples are abbreviated as followak biochar (OK), activated oak biochar (OK-A), hydrogel composite (HG) and activated hydrogel composite (HG-A)

bond to the materials. At a larger distance (i.e., to the right of the first peak)), a smaller peak indicates the presence of a second backscattering signal. Well resolved two peaks in the magnitude of Fourier Transformed EXAFS signal could suggest that strontium forms direct bonds with activated oak wood biochar via oxygen and carbon atoms, essentially confirming presence of an inner sphere complexation at pH 7. The system was buffered during uptake since the pH-dependent nature of strontium binding is well known [6, 7, 24]. Oftentimes other strontium adsorbents exhibit little or no second shell signal at circumneutral pH indicating outer sphere complexation [24–26] in contrast to the adsorbents in this study.

Derived coordination numbers and atomic distances are displayed in Table 3. Both activated HG-A and unactivated HG hydrogel show a slightly larger second shell carbon (Sr–C) signal compared with activated biochar OK-A,

indicating a higher degree of inner sphere binding in both hydrogel bead samples. Sr–O distances are consistently 2.57 ± 0.01 Å for the HG, HG-A and OK-A samples. This is marginally shorter than most Sr–O distances reported, yet do fall within the reported range of 2.55–2.64 Å [5, 7, 22, 24]. Sr–C distances reported in this study are intermediate within the range of organic Sr–C distances (3.05–3.8 Å) reported in crystallographic diffraction studies [24–27]. Sr–C distance in a carboxylate bidentate binding can be as short as 3.05 Å [24], while an oxalate bidentate binding mode yields Sr–C distance of around 3.3–3.45 Å [30] and monodentate binding typically yields Sr–C distance above 3.4 Å [24, 25, 27]. Both hydrogels HG and HG-A as well as activated biochar OK-A display Sr–C distances 3.0–3.8 Å, suggesting the composition of the oxygen functional groups through which they are binding are a combination of carboxylate bidentate and monodentate groups such as hydroxyls, lactones and carbonyls. This is consistent with the egg-box model of group II binding to alginate [31], [32] which describes a penta-dentate binding of strontium to a combination of carboxylate and hydroxylate moieties. These distances are also consistent with known oxygen functionality the biochar component, which is known to contain a mix of carboxylate, hydroxyl and other oxygen moieties. Therefore, the binding environment of strontium in activated oak wood biochar and its hydrogel composites is best described by a combination of bidentate and monodentate binding with oxygen surface functional groups.

Conclusions

Activated hydrogel alginate-biochar composite beads are a sustainable and low-cost material for radionuclide remediation. They are effective at removal of strontium at environmentally relevant pH and are compatible with use in environmental systems. Strontium batch uptake experiments were conducted deriving a maximum strontium uptake capacity of 108.5 mg g⁻¹ for activated hydrogel, significantly higher than an unactivated control hydrogel or activated biochar alone. EXAFS fitting revealed the inner sphere binding of strontium to all three adsorbents—activated particulate biochar, unactivated hydrogel and activated hydrogel composites, indicating strong and irreversible binding of strontium to all three of these materials. This study is the first to report direct evidence for an inner sphere binding of strontium on biopolymers. Hydrogel encapsulation of activated biochar combines the enhanced uptake capacity of activated biochar in a monolithic composite material. Further uptake studies are required to more accurately model uptake and binding bulk behaviour.

Fig. 2 Normalised EXAFS spectra (left) and Fourier transform magnitude spectra (right) for samples and reference sample, collected at 77 K

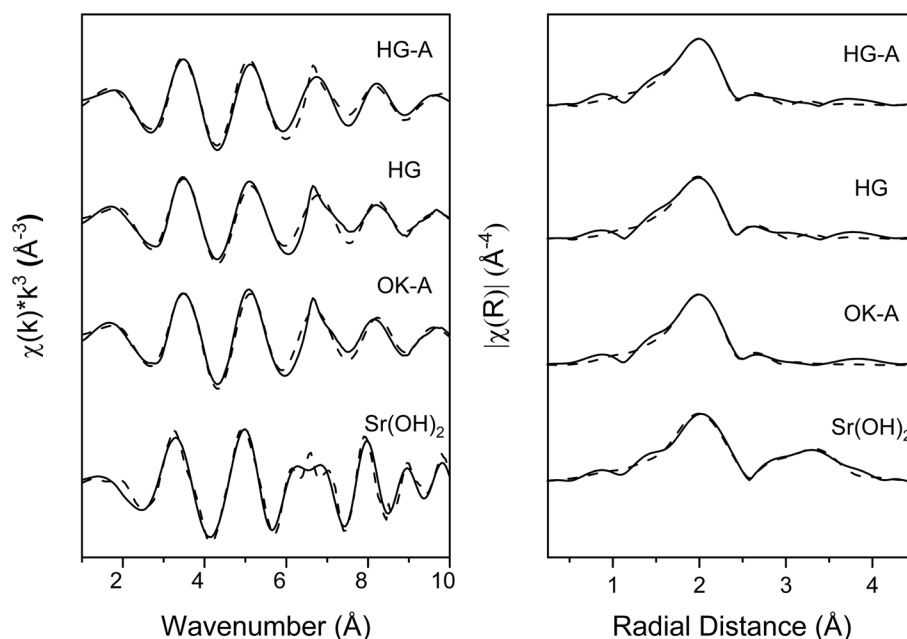


Table 3 EXAFS fitting parameters

Sample	Scatterer shell	Coordination number	R (Å)	ΔE_0 (eV)	$\sigma^2 * 10^{-3}$ (Å ²)
HG-A	Sr–O	8.8 ± 0.99	2.57 ± 0.01	3.03 ± 0.95	13.4 ± 1.6 ^a
	Sr–C	3.4 ± 1.34	3.37 ± 0.04		
HG	Sr–O	7.7 ± 0.91	2.56 ± 0.01	3.25 ± 0.95	12.8 ± 1.7 ^a
	Sr–C	4.0 ± 1.22	3.38 ± 0.04		
OK-A	Sr–O	9.1 ± 0.93	2.57 ± 0.01	3.04 ± 0.99	12.9 ± 1.5 ^a
	Sr–C	3.0 ± 1.37	3.30 ± 0.04		
Sr(OH) ₂	Sr–O	13.0 ± 1.27	2.62 ± 0.01	1.38 ± 0.71	15.0 ± 1.8
	Sr–Sr	3.9 ± 1.18	3.71 ± 0.01		8.1 ± 2.7

S_0^2 , the amplitude reduction factor, is fixed to 1 [18]. $^a\sigma^2$, the Debye–Waller factor, in the Sr–C shell is fixed to the value for each sample Sr–O shell respectively

Supplementary Information The online version contains supplementary material available at <https://doi.org/10.1007/s10967-022-08613-6>.

Acknowledgements Thanks to B18 beamline scientists at Diamond Light Source as well as Dr Adrian Cunliffe and Karine Alvez Thorne-Alvarez at the University of Leeds. This work was supported by a doctoral training partnership (DPT) studentship from the Engineering and Physical Science Research Council (EPSRC).

Open Access This article is licensed under a Creative Commons Attribution 4.0 International License, which permits use, sharing, adaptation, distribution and reproduction in any medium or format, as long as you give appropriate credit to the original author(s) and the source, provide a link to the Creative Commons licence, and indicate if changes were made. The images or other third party material in this article are included in the article's Creative Commons licence, unless indicated otherwise in a credit line to the material. If material is not included in the article's Creative Commons licence and your intended use is not permitted by statutory regulation or exceeds the permitted use, you will need to obtain permission directly from the copyright holder. To view a copy of this licence, visit <http://creativecommons.org/licenses/by/4.0/>.

References

- Musilli S, Nicolas N, El Ali Z et al (2017) DNA damage induced by strontium-90 exposure at low concentrations in mesenchymal stromal cells: the functional consequences. *Sci Rep* 7:1–15. <https://doi.org/10.1038/srep41580>
- Gould JM, Sternglass EJ, Sherman JD et al (2000) Strontium-90 in deciduous teeth as a factor in early childhood cancer. *McDonnell and Joseph J. Mangano Int J Health Serv* 30:515–539
- Sahai N, Carroll SA, Roberts S, O'Day PA (2000) X-ray absorption spectroscopy of strontium(II) coordination. II. Sorption and precipitation at kaolinite, amorphous silica, and goethite surfaces. *J Colloid Interface Sci* 222:198–212. <https://doi.org/10.1006/jcis.1999.6562>
- Fuller AJ, Shaw S, Peacock CL et al (2016) EXAFS study of Sr sorption to illite, goethite, chlorite, and mixed sediment under hyperalkaline conditions. *Langmuir* 32(12):2937–2946. <https://doi.org/10.1021/acs.langmuir.5b04633>
- Cleary A, Lloyd JR, Newsome L et al (2019) Bioremediation of strontium and technetium contaminated groundwater using

- glycerol phosphate. *Chem Geol* 509:213–222. <https://doi.org/10.1016/j.chemgeo.2019.02.004>
6. Murphy EM, Zachara JM (1995) The role of sorbed humic substances on the distribution of organic and inorganic contaminants in groundwater. *Geoderma* 67:103–124. [https://doi.org/10.1016/0016-7061\(94\)00055-F](https://doi.org/10.1016/0016-7061(94)00055-F)
 7. Shen Y, Chapelle FH, Strom EW, Benner R (2015) Origins and bioavailability of dissolved organic matter in groundwater. *Biogeochemistry* 122:61–78. <https://doi.org/10.1007/s10533-014-0029-4>
 8. Ellis D, Bouchard C, Lantagne G (2000) Removal of iron and manganese from groundwater by oxidation and microfiltration. *Desalination* 130:255–264. [https://doi.org/10.1016/S0011-9164\(00\)00090-4](https://doi.org/10.1016/S0011-9164(00)00090-4)
 9. Griebler C, Lueders T, Mu HZ (2009) Microbial biodiversity in groundwater ecosystems. *Freshw Biol.* 54:649–677. <https://doi.org/10.1111/j.1365-2427.2008.02013.x>
 10. Mikhaylin S, Bazinet L (2016) Fouling on ion-exchange membranes: classification, characterization and strategies of prevention and control. *Adv Colloid Interface Sci* 229:34–56. <https://doi.org/10.1016/j.cis.2015.12.006>
 11. Artham T, Sudhakar M, Venkatesan R et al (2009) Biofouling and stability of synthetic polymers in sea water. *Int Biodeterior Biodegrad* 63:884–890. <https://doi.org/10.1016/j.ibiod.2009.03.003>
 12. Ching SH, Bansal N, Bhandari B (2017) Alginate gel particles—a review of production techniques and physical properties. *Crit Rev Food Sci Nutr* 57:1133–1152. <https://doi.org/10.1080/10408398.2014.965773>
 13. Kelly SD, Kemner KM, Fein JB et al (2002) X-ray absorption fine structure determination of pH-dependent U-bacterial cell wall interactions. *Geochim Cosmochim Acta* 66:3855–3871. [https://doi.org/10.1016/S0016-7037\(02\)00947-X](https://doi.org/10.1016/S0016-7037(02)00947-X)
 14. Mishra B, Boyanov MI, Bunker BA et al (2009) An X-ray absorption spectroscopy study of Cd binding onto bacterial consortia. *Geochim Cosmochim Acta* 73:4311–4325. <https://doi.org/10.1016/j.gca.2008.11.032>
 15. Bots P, Comarmond MJ, Payne TE et al (2021) Emerging investigator series: a holistic approach to multicomponent EXAFS: Sr and Cs complexation in clayey soils. *Environ Sci Process Impacts* 23:1101–1115. <https://doi.org/10.1039/d1em00121c>
 16. Kaçan E, Kütahyalı C (2012) Adsorption of strontium from aqueous solution using activated carbon produced from textile sewage sludges. *J Anal Appl Pyrolysis* 97:149–157. <https://doi.org/10.1016/j.jaap.2012.06.006>
 17. Akkaya G, Güzel F, Say H (2017) Optimal oxidation with nitric acid of biochar derived from pyrolysis of weeds and its application in removal of hazardous dye methylene blue from aqueous solution. *J Clean Prod* 144:260–265. <https://doi.org/10.1016/j.jclepro.2017.01.029>
 18. Jang J, Mirana W, Divine SD et al (2018) Rice straw-based biochar beads for the removal of radioactive strontium from aqueous solution. *Sci Total Environ* 615:698–707. <https://doi.org/10.1016/j.scitotenv.2017.10.023>
 19. Langmuir I (1918) Adsorption of gases on glass mica and platinum. *J Am Chem* 40(9):1361–1403
 20. Gok C, Gerstmann U, Aytas S (2013) Biosorption of radiostrontium by alginate beads: application of isotherm models and thermodynamic studies. *J Radioanal Nucl Chem* 295:777–788. <https://doi.org/10.1007/s10967-012-1838-3>
 21. Parkman RH, Charnock JM, Livens FR, Vaughan DJ (1998) A study of the interaction of strontium ions in aqueous solution with the surfaces of calcite and kaolinite. *Geochim Cosmochim Acta* 62:1481–1492. [https://doi.org/10.1016/S0016-7037\(98\)00072-6](https://doi.org/10.1016/S0016-7037(98)00072-6)
 22. Zhang X, Wang L, Weng L, Deng B (2020) Strontium ion substituted alginate-based hydrogel fibers and its coordination binding model. *J Appl Polym Sci* 137:1–9. <https://doi.org/10.1002/app.48571>
 23. Cao L, Lu W, Mata A et al (2020) Egg-box model-based gelation of alginate and pectin: a review. *Carbohydr Polym* 242:116389. <https://doi.org/10.1016/j.carbpol.2020.116389>
 24. Stahl K, Shim I, Christgau S (2009) Structures of strontium diformate and strontium fumarate. A synchrotron powder diffraction study research papers. *Acta Crystallogr Sect B Struct Sci.* <https://doi.org/10.1107/S0108768109023489>
 25. Liao W (2004) b-Strontium carbodiimide. *Acta Crystallogr A.* <https://doi.org/10.1107/S1600536804023244>
 26. Vanhoyland G, Van BMK, Mullens J, Van PLC (2007) Structure determination of anhydrous acid strontium oxalate by conventional X-ray powder diffraction. *Powder Diffr* 16:224–226. <https://doi.org/10.1154/1.1401199>
 27. Thorpe CL, Lloyd JR, Law GTW et al (2012) Strontium sorption and precipitation behaviour during bioreduction in nitrate impacted sediments. *Chem Geol* 306–307:114–122. <https://doi.org/10.1016/j.chemgeo.2012.03.001>

Publisher's Note Springer Nature remains neutral with regard to jurisdictional claims in published maps and institutional affiliations.